# Pentraxin-3 Is a TSH-Inducible Protein in Human Fibrocytes and Orbital Fibroblasts

Hao Wang, Stephen J. Atkins, Roshini Fernando, Rui-Li Wei, and Terry J. Smith

Departments of Ophthalmology and Visual Sciences (H.W., S.J.A., R.F., T.J.S.), University of Michigan Medical School, Ann Arbor, Michigan 48105; Department of Ophthalmology (H.W., R.-L.W.), Shanghai Changzheng Hospital, Second Military Medical University, 200003 Shanghai, China; and Division of Metabolism (T.J.S.), Endocrinology, and Diabetes, University of Michigan Medical School, Ann Arbor, Michigan 48105

CD34$^+$ fibrocytes are bone marrow–derived monocyte progenitor cells that traffic to sites of tissue injury and repair. They putatively infiltrate the orbit in thyroid-associated ophthalmopathy where they appear to transition into CD34$^+$ orbital fibroblasts (OFs) that interact with residential CD34$^-$ fibroblasts. A unique phenotypic attribute of fibrocytes and CD34$^+$ OFs is their expression of the functional thyrotropin receptor (TSHR) and other "thyroid-specific" proteins. When activated through TSHR, fibrocytes express a number of cytokines and other inflammatory genes. Here we sought to determine whether pentraxin-3 (PTX-3), an acute-phase protein involved in inflammation and autoimmunity, might be induced by TSH in fibrocytes and OFs. These cells were collected from patients with Graves disease and healthy individuals. PTX-3 mRNA levels were determined by real-time PCR, protein was determined by ELISA and Western blot, and PTX-3 gene promoter activity was assessed with reporter assays. PTX-3 expression was induced by TSH in both cell types, regardless of the health status of the donor and was a consequence of increased steady-state PTX-3 mRNA levels. M22, a TSHR-activating monoclonal antibody, also induced PTX-3. The induction could be attenuated by dexamethasone and by IGF-I receptor–blocking antibodies, teprotumumab and 1H7. TSH effects were mediated through phosphatidylinositol 3-kinase/AKT, mammalian target of rapamycin/p70$^{s6k}$, Janus tyrosine kinase 2 pathways, and enhanced PTX-3 mRNA stability. These findings indicate that PTX-3 is a TSH target gene, the expression of which can be induced in fibrocytes and OFs. They suggest that PTX-3 might represent a previously unidentified nexus between the thyroid axis and the mechanisms involved in tissue remodeling. (***Endocrinology* 156: 4336–4344, 2015)**

Graves disease (GD) is an autoimmune syndrome in which the thyroid overproduces thyroid hormones as a consequence of thyroid-stimulating immunoglobulin (TSI) activating the TSH receptor (TSHR) displayed on thyroid epithelial cells (1). A frequent manifestation of GD is thyroid-associated ophthalmopathy (TAO), in which orbital connective tissues and extraocular muscles become inflamed and undergo remodeling (2, 3). The molecular mechanisms underlying TAO have been only partially elucidated, resulting in suboptimal therapy (4). Most investigators in the field currently believe that TSIs play a role in driving the pathogenesis of TAO.

Earlier studies from several laboratories have suggested strongly that orbital fibroblasts (OFs) inhabiting the adipose/connective tissues are primarily targeted in TAO (4–6). OFs can be divided into multiple subsets based on the surface markers they display, their divergent responses to molecular cues, and their distinct capacities for terminal differentiation (7). A subset of OFs uniquely derived from the TAO orbit (GD-OFs), display the bone marrow pro-

ISSN Print 0013-7227 ISSN Online 1945-7170
Printed in USA

Received May 5, 2015. Accepted August 13, 2015.
First Published Online August 19, 2015

Abbreviations: AKTi, AKT inhibitor; bTSH, bovine TSH; CRP, C-reactive protein; Dex, dexamethasone; DRB, 5,6-dichloro-$\beta$-D-ribofuranosylbenzimidazole; FBS, fetal bovine serum; GAPDH, glyceraldehyde-3-phosphate dehydrogenase; GD, Graves disease; IGF-IR, IGF-I receptor; JAK2, Janus kinase 2; mTOR, mammalian target of rapamycin; nt, nucleotides; OF, orbital fibroblast; PBMC, peripheral blood mononuclear cell; PI3K, phosphatidylinositol 3-kinase; PTX-3, pentraxin-3; SAP, serum amyloid P; TAO, thyroid-associated ophthalmopathy; TSHR, TSH receptor; TSI, thyroid-stimulating immunoglobulin.

genitor phenotype $CD34^+CXCR4^+Col1^+$, suggesting but not proving that they derive from circulating $CD34^+$ fibrocytes (8, 9). Fibrocytes can migrate to sites of tissue injury and inflammation and participate in tissue remodeling (10–12). They express both leukocyte and fibroblast surface antigens (11). Our laboratory group has actively investigated the phenotype of fibrocytes and derivative $CD34^+$ OFs in the context of TAO (13–15). Fibrocytes cultivated from circulating peripheral blood mononuclear cells (PBMCs) express remarkably high levels of functional TSHR; however, the receptor is dramatically downregulated in GD-OFs (8, 9, 13). When stimulated by TSH and TSHR-activating antibodies, fibrocytes produce several cytokines (16). Based on these earlier findings, we postulate that fibrocytes may link innate immunity and orbital connective tissue activation.

Long pentraxin-3 (PTX-3) is an acute-phase protein belonging to the pentraxin family (17). This family includes C-reactive protein (CRP) and serum amyloid P (SAP) (18). Unlike hepatic production of CRP, PTX-3 is expressed by several different tissues and cell types (17, 19–21) during tissue injury and stress. PTX-3 can be induced by Toll-like receptor agonists or proinflammatory cytokines (20). PTX-3 is also produced constitutively and stored in the $lactoferrin^+$ granules of neutrophils (22). It may be a biomarker for inflammation and innate immune activity (23). With regard to GD, Planck et al (24) found elevated PTX-3 mRNA levels in orbital adipose tissues from active but not stable TAO.

In the current report, we demonstrate that PTX-3 is induced dramatically in fibrocytes and OFs by bovine TSH (bTSH), which rapidly up-regulates the steady-state levels of PTX-3 mRNA and PTX-3 protein. The induction can be attenuated by dexamethasone (Dex). This induction is a consequence of stabilization of PTX-3 mRNA. Thus, PTX-3 appears to represent a heretofore unrecognized TSH-inducible protein in fibrocytes and OFs.

## Materials and Methods

### Materials

DMEM (catalog no. 11965–092), fetal bovine serum (FBS) (catalog no. 16–000-044), and penicillin-streptomycin mixture (catalog no. 15–140-122) were purchased from Life Technologies. bTSH (catalog no. 609–385), LY294002 (phosphatidylinositol 3-kinase (PI3K) inhibitor; catalog no. 440–202), AG490 (Janus kinase 2 [JAK2] inhibitor; catalog no. 658–401), and AKT inhibitor (AKTi) (catalog no. 124–005) came from EMD Millipore. Rapamycin (catalog no. R8781) and Dex (catalog no. D4902) were from Sigma-Aldrich. Anti-PTX-3 antibody (catalog no. ALX-210–365-C050) came from Enzo. M22 (catalog no. 5600) was from Kronus. Teprotumumab (RV001) was a gift from River Vision. 1H7 (catalog no. 555–998) came from BD Biosciences. Anti-phospho-AKT (Ser473) (catalog no. 4058), anti-AKT (catalog no. 9272), anti-phospho-$p70^{S6K}$ (Thr389) (catalog no. 9205), and anti-$\beta$-actin (catalog no. 3700) antibodies came from Cell Signaling Technology. Anti-$p70^{S6K}$ (catalog no. sc-8418), anti- phospho-JAK2 (Tyr1007/Tyr1008) (catalog no. sc-16–566-R), and anti-JAK2 (catalog no. sc-34–479) antibodies were from Santa Cruz Biotechnology. 5,6-Dichloro-$\beta$-D-ribofuranosylbenzimidazole (DRB) (catalog no. 10–010-302) came from Cayman Chemical.

### Cell culture

Fibrocytes were isolated from PBMCs as described previously (10) from patients with GD and TAO (n = 5 females) or healthy donors (n = 16). All subjects were uniformly euthyroid at the time of study participation and were not taking corticosteroids. Samples were collected after informed consent was obtained. These activities have been approved by the institutional review board of the University of Michigan Health System. Blood was centrifuged over Ficoll-Paque Plus (catalog no. 17–1440-03; GE). A total of $10^7$ PBMCs were inoculated in each well of 6-well plates and covered with DMEM containing 10% FBS, 2 mM glutamine, sodium pyruvate (110 mg/mL), 1% penicillin/streptomycin, and 4.5% glucose. Unattached cells were discarded by gentle aspiration after 7 days, and monolayers were incubated for an additional 3 to 5 days before use. Culture purity was verified to be >90% fibrocytes by flow cytometric analysis.

GD-OFs were generated from intraconal fat obtained as surgical waste during orbital decompressions for severe TAO (n = 3, 1 male and 2 female donors). The donors with TAO were euthyroid, had uniformly entered the stable (inactive) phase of TAO, and had not been exposed to high-dose corticosteroids. None had undergone external beam radiation. H-OF were derived from 1 male and 2 female otherwise healthy donors undergoing either exenteration for intraocular disease (n = 1) or cosmetic surgery (n = 2). OFs were allowed to proliferate as described previously (25), and monolayers were covered with DMEM. They were maintained in a 37°C, humidified, 5% $CO_2$ environment. Culture strains were used between the 5th and 10th passages from initial plating, an interval during which we have determined that cell phenotypes remain constant. The medium was changed every 3 to 4 days.

### RNA isolation and quantitative RT-PCR

Cultures were shifted to medium containing 1% FBS for 12 hours before the treatments indicated in the figure legends. Cellular RNA was extracted with the Aurum total RNA Mini Kit (catalog no. 732–6820; Bio-Rad). RNA was then reverse-transcribed using a QuantiTec reverse transcription kit (catalog no. 205310; QIAGEN). Quantitative RT-PCR was carried out with iQ SYBR Green Supermix (catalog no. 170–8882; Bio-Rad) in a Bio-Rad CFX96 thermocycler. PCRs were performed in triplicate and glyceraldehyde-3-phosphate dehydrogenase (GAPDH) was used as the housekeeping gene control. The primers used were as follows: PTX-3, forward 5′-GTGCTCTCTGGTCTGCAGTG-3′ and reverse 5′-GTCGTCCGTGGCTTGCAG-3′; TSHR, forward 5′-AGCCACTGCTGTGCTTTTAAG-3′ and reverse 5′-CCAAAACCAATGATCTCATCC-3′; and GAPDH, forward 5′-TTGCCATCAATGACCCCTA-3′ and reverse 5′-CGCCCCACTTGATTTTGG-3′. Reactions were performed at 95°C for 3 minutes, 40 cycles at 95°C for 15 seconds, and 62.5°C for 40 seconds.

### PTX-3 mRNA stability assay

Confluent fibrocyte cultures were pretreated with bTSH for 6 hours. DRB (50 $\mu$M) was added without or with bTSH at time 0, and RNA was harvested at the times indicated along the abscissa in Figure 6B. Samples were subjected to quantitative RT-PCR. The $t_{1/2}$ values were calculated using the comparative critical threshold method. Normalized data from $t = 0$ were arbitrarily set as 100%. Data were graphed as a best-fit line.

### SDS-PAGE and Western blotting

Cell lysates were prepared using 50 $\mu$L of lysis buffer [50 mM HEPES, 150 mM NaCl, 15 mM $MgCl_2$,1 mM 4-(2-hydroxy-

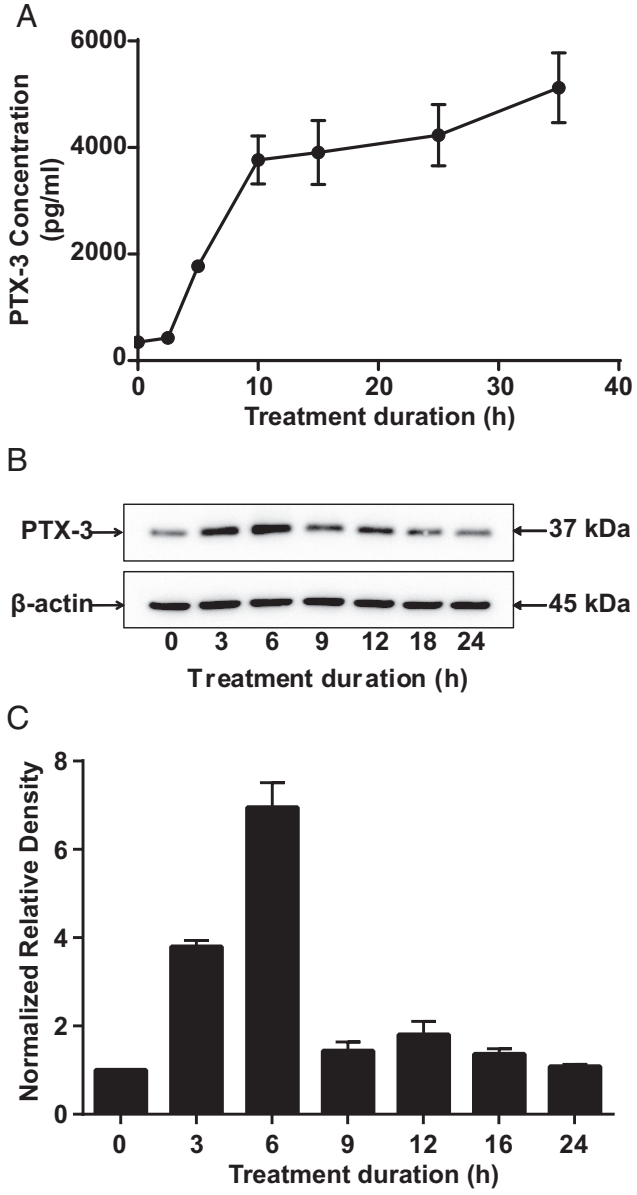


**Figure 1.** Time course of PTX-3 protein induction in fibrocytes by bTSH. Confluent cultures were incubated without or with bTSH (5 mIU/mL) for the intervals indicated along the abscissas. A, Medium was collected and subjected to a PTX-3–specific ELISA. Data are expressed as means ± SD of triplicates from 3 independent experiments. $P < .05$ compared with baseline. B, Cellular protein was extracted for Western blot analysis. C, Bands from B were quantified by densitometric analysis.

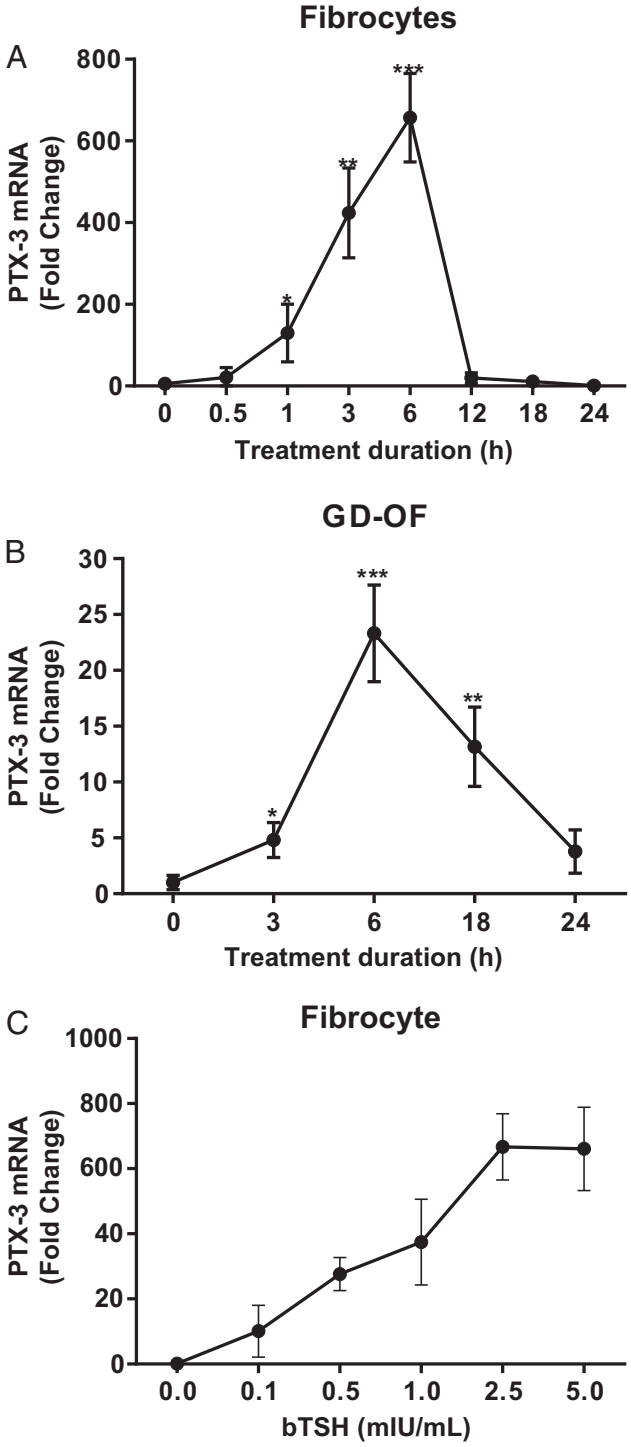


**Figure 2.** Time course of PTX-3 mRNA induction in fibrocytes (A) and GD-OFs (B) by bTSH. Confluent cells from a single healthy fibrocyte donor and from a single GD-OF donor were shifted to medium containing 1% FBS for 12 hours, and then bTSH (5 mIU/mL) was added for the intervals indicated along the abscissas. C, Graded concentrations of bTSH indicated along the abscissa were added to culture medium for 6 hours. Total RNA was extracted, reverse transcribed, and subjected to RT-PCR for PTX-3 mRNA. Data are expressed as means ± SD of triplicates from 3 independent experiments. *, $P < .05$; **, $P < .01$; ***, $P < .001$; compared with baseline.

ethyl)-1-piperazineethanesulfonic acid, 1 mM $NaHPO_4$, 1 mM dithiothreitol, 1 mM sodium orthovanadate, 1% Triton X-100, 0.05% SDS, 10 μg/mL aprotinin, and 10 μg/mL leupeptin]. Protein concentrations were determined, and equal amounts were loaded on SDS-PAGE, running at 80 V for 15 minutes and then at 120 V for 45 minutes. Separated proteins were transferred to polyvinylidene difluoride membranes, which were incubated with 5% nonfat milk in 1× Tris-buffered saline–Tween 20 with primary antibodies overnight. Membranes were washed and then incubated with horseradish peroxidase–conjugated polyclonal anti-rabbit secondary antibodies for 2 hours at room temperature. Signals were detected using an enhanced chemiluminescence kit (catalog no. 32106; Thermo Scientific). The bands were visualized in FluorChem E (catalog no. 92–14860-00; ProteinSimple). Images were subjected to densitometry performed with Image-Pro Plus (version 6.0; Media Cybernetics).

### ELISA

PTX-3 protein was quantified with a PTX-3 (Human) OmniKine ELISA Kit (catalog no. OK-0346; Assay Biotechnology), according to the manufacturer's instructions. Details of the assay sensitivity and specificity can be found on the supplier's website.

### Cloning of the human PTX-3 promoter, transient transfections, and luciferase reporter assays

PTX-3 promoter fragments were amplified by PCR and subcloned into the pGL3 vector. To clone deletional fragments, the following primers were used. Forward primers were −1399/+3 nucleotides (nt), 5′-CCCGGGGGATCTCCCTTCTAACTCTCCAC-3′; −1125/+3 nt, 5′-CTAAGTTTACTTTTAAAACATGATCCTTGC-3′; −859/+3 nt, 5′-AGCCTGGCTAACATGGTGAAACCCTGTCTCT-3′; −589/+3 nt, 5′-TTGACTTTCAGAGCCATAACTATTCTTAAT-3′; −334/+3 nt, and 5′-GAACAGTAGAAGCCCAGTTTCTCTCCTCTTT-3′. The reverse primer was 5′-CTAGCACGCGTAAGAGCTCGGTAC-3′. The constructs were transfected into 80% confluent fibrocytes, using an Amaxa Human CD34 Cell Nucleofector Kit (catalog no. VPA-1003; Lonza) as described previously (13). *Renilla* luciferase–encoding plasmid phRL-TK was cotransfected as a control. After 24 hours, monolayers were treated with nothing or bTSH (5 mIU/mL) for 2 hours, and luciferase activities were determined by a dual-luciferase reporter assay (Promega). All transfection assays were performed in triplicate. LumiCount data were normalized to their *Renilla* transfection controls.

### Statistics

Statistical analysis was performed using a two-tailed Student *t* test. Data are expressed as the means ± SD. All experiments were conducted in triplicate and performed at least 3 times.

## Results

### PTX-3 is a TSH-inducible molecule in fibrocytes

To determine whether bTSH (5 mIU/mL) could induce PTX-3 expression, fibrocytes, in this case from a healthy donor, were incubated in its absence or presence for graded intervals. Culture medium was collected at the time points indicated along the abscissa and subjected to a PTX-3 ELISA (Figure 1A). PTX-3 levels rapidly increased after exposure to bTSH. The protein was detectable at relatively low levels at baseline, but at 35 hours, the duration of the study, PTX-3 levels were 14.7-fold above baseline ($P < .05$). The time course for induction of PTX-3 in OFs was similar to that in fibrocytes (data not shown). Cell layers were analyzed by Western blotting for PTX-3. The protein resolves as a band at 37 kDa, which was readily detectable at baseline, peaked at 6 hours with a 6.9-fold increase, and rapidly returned to baseline by 9 hours (Figure 1, B and C).

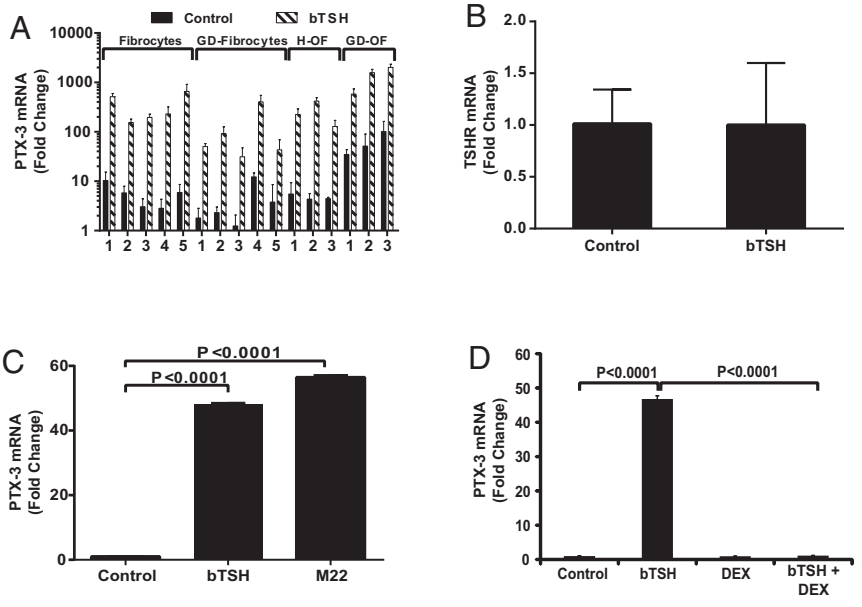


**Figure 3.** A, TSH induction of PTX-3 mRNA in multiple strains of fibrocytes, GD-OFs, and H-OFs. Five strains of fibrocytes from patients with GD, 5 from healthy donors, and 3 strains each of GD-OFs and H-OFs were treated with nothing (control) or bTSH (5 mIU/mL) for 6 hours. Total RNA was extracted and subjected to RT-PCR for PTX-3 mRNA. B, Fibrocytes were treated with nothing (control) or bTSH 5 mIU/mL for 72 hours, monolayers were harvested, and RNA was extracted and subjected to RT-PCR for TSHR mRNA. C, Fibrocytes were treated with nothing, bTSH, or M22 (2 μg/mL) for 6 hours, and then RNA was subjected to RT-PCR for PTX-3 mRNA. D, Fibrocyte cultures were treated with nothing, bTSH, or Dex (10 nM) for 6 hours. RNA was subjected to RT-PCR for PTX-3 mRNA. Data are expressed as means ± SD of triplicates from 3 independent experiments. *P* values are as indicated.

### PTX-3 induction by TSH is mediated at a pretranslational level

Confluent fibrocytes and GD-OFs were treated without or with bTSH (5 mIU/mL) for graded inter-

vals, and cellular RNA was subjected to RT-PCR. As demonstrated in Figure 2, PTX-3 mRNA was dramatically increased in both fibrocytes (Figure 2A) and GD-OFs (Figure 2B) in a time-dependent manner with maximal induction occurring at 6 hours ($P < .001$ vs control). The induction was considerably more transient in fibrocytes in which mRNA levels returned to baseline at 12 hours. In contrast, PTX-3 mRNA in GD-OF remained elevated at 24 hours when it was 3.8-fold above baseline. The induction was concentration-dependent, was detectable at 0.1 mIU/mL, the lowest bTSH concentration tested, and was maximal at 2.5 mIU/mL (Figure 2C).

Fibrocytes exhibit substantial constitutive PTX-3 mRNA expression in cultures from 5 different patients with GD and 5 healthy donors in addition to 3 strains each of GD-OFs and H-OFs (Figure 3A). The basal levels in GD-OFs appear to be higher than those in H-OFs ($P < .05$). bTSH induced PTX-3 mRNA in all strains of fibrocytes and OFs. The magnitude of induction ranged from 11- to 110-fold and was not significantly different in fibrocytes from healthy donors and those with GD. Thus, the results obtained from orbital fibroblasts of patients with TAO, ie GD-OFs and those from healthy individuals (H-OFs) were identical. The effects of bTSH (5 mIU/mL) on TSHR expression were assessed by treating monolayers for 72 hours and assessing the levels of TSHR mRNA. The treatment failed to alter the expression of the receptor (Figure 3B), suggesting that an up-regulation of TSHR was not involved in the induction of PTX-3.

M22, a monoclonal activating antibody targeting TSHR, was examined for its effect on PTX-3 expression in fibrocytes. bTSH (5 mIU/mL) and M22 (2 $\mu$g/mL) induced PTX-3 mRNA equivalently after 6 hours (Figure 3C). The effects of M22 could be detected at the lowest concentration tested, 100 ng/mL (control, $0.47 \pm 0.13$; M22, $1.00 \pm 0.27$; $P < .05$). These results imply that TSI might mimic the actions of TSH on fibrocytes in the context of GD.

## Dex and IGF-I receptor (IGF-IR) blocking antibodies attenuate TSH-induced PTX-3 expression in fibrocytes

Corticosteroids represent a mainstay among anti-inflammatory therapeutic agents in active TAO (4). To investigate whether the specific glucocorticoid, Dex, can block the induction by bTSH of PTX-3 mRNA, fibrocytes were treated with nothing or the steroid (10 nM) alone or in combination with bTSH (5 mIU/mL) for 6 hours. Dex substantially inhibited the up-regulation of PTX-3 by bTSH (97.6% inhibition; $P < .0001$ compared to bTSH alone) (Figure 3D).

We previously reported that teprotumumab, an IGF-IR blocking monoclonal antibody, can attenuate the downstream actions of TSH in fibrocytes (26). Further, that drug is currently being studied in a clinical trial for severe, active TAO (http://clinicaltrials.gov/show/NCT01868997). Whether IGF-IR blocking monoclonal antibodies might inhibit TSH-induced PTX-3 expression in fibrocytes was next addressed. Confluent fibrocytes were pretreated with nothing or RV001 (50 $\mu$g/mL) or 1H7, another anti-IGF-IR blocking antibody (10 $\mu$g/mL) for 16 hours. They were then treated with nothing or bTSH (5 mIU/mL) for 6 hours. Teprotumumab and 1H7 significantly attenuated the induction by bTSH of PTX-3 mRNA by 79.8% ($P < .05$) and 47.9% ($P < .05$), respectively (Figure 4A). Thus, the actions of bTSH on PTX-3 expression appear to involve IGF-IR activity. The effect of IGF-I on the induction of PTX-3 by bTSH was next determined by cotreating fibrocyte cultures for 6 hours with the agents alone and in combination (Figure 4B). Addition of IGF-I failed to enhance the magnitude of the induction by bTSH.

## Multiple signal transduction pathways are involved in the induction by TSH of PTX-3

Signaling downstream from TSHR in fibrocytes is relatively complex. Phosphoinositide-dependent protein kinase 1, protein kinase C, and AKT appear to play roles in

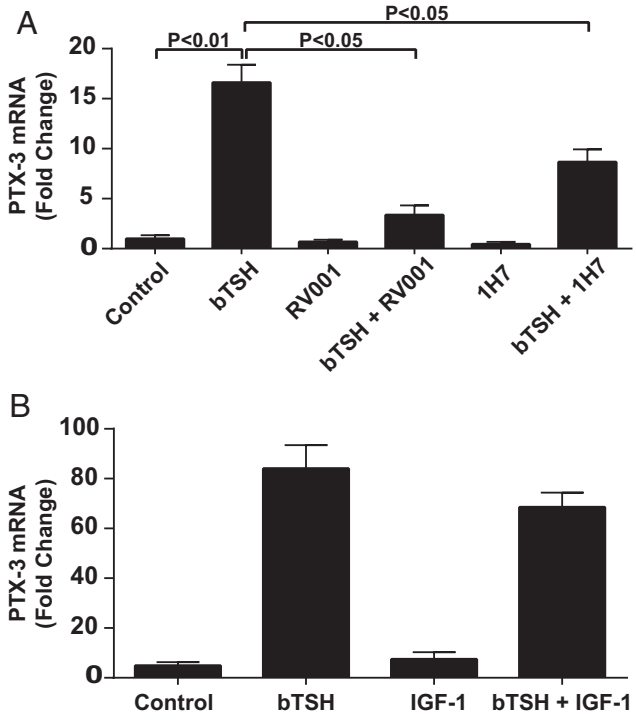


**Figure 4.** A, Anti-IGF-IR blocking antibodies, RV001 and 1H7, attenuate the induction by TSH of PTX-3 in fibrocytes. Confluent cultures were pretreated with nothing, RV001 (50 $\mu$g/mL) or 1H7 (10 $\mu$g/mL) for 16 hours and then incubated without or with bTSH (5 mIU/mL) for an additional 6 hours. Cellular RNA was subjected to RT-PCR for PTX-3 mRNA. B, Confluent fibrocyte cultures were treated with nothing, bTSH (5 mIU/mL), IGF-I (10 ng/mL), or the combination of bTSH and IGF-I for 6 hours. Cellular RNA was subjected to RT-PCR of PTX-3 mRNA. Data are expressed as mean ± SD of triplicate replicates.

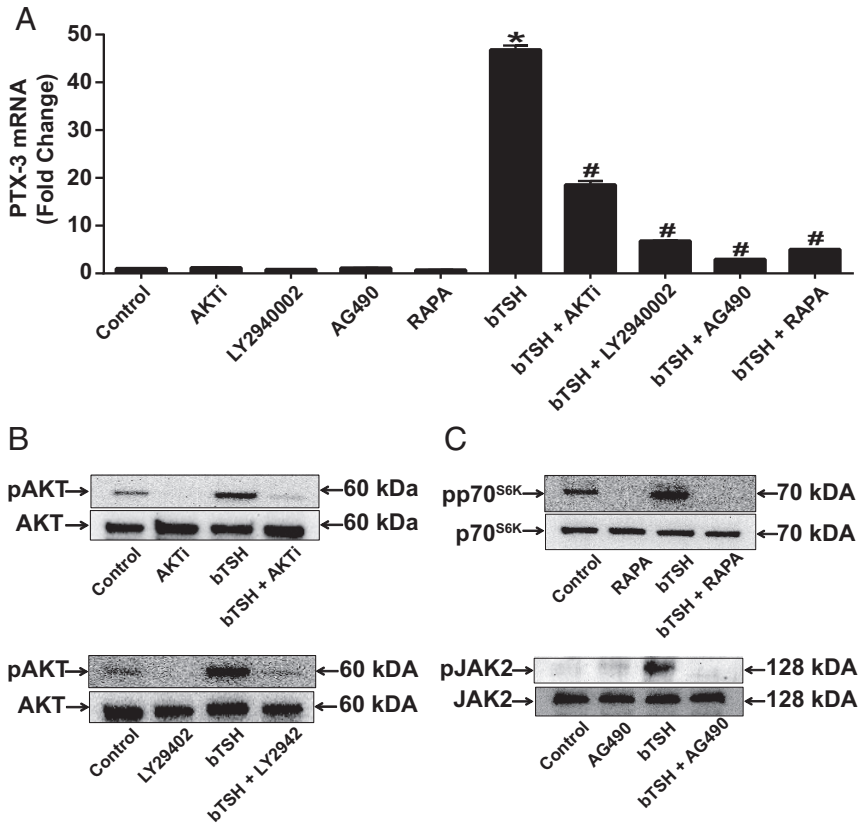


**Figure 5.** A, Fibrocytes were pretreated with nothing or AKTi (1 $\mu$M), LY294002 (10 $\mu$M), AG490 (75 $\mu$M), rapamycin (RAPA) (20 nM) for 1 hour before incubation with bTSH (5 mIU/mL) for 6 hours. RNA was subjected to RT-PCR for PTX3 mRNA. Data are expressed as means ± SD of triplicates from 3 independent experiments. *, $P < .0001$ compared with control; **#**, $P < .0001$ compared with bTSH alone. B and C, Cultures were pretreated as in A and then treated with bTSH (5 mIU/mL) for 90 minutes. Cell lysates were subjected to Western blot analysis of AKT, pAKT, JAK2, pJAK2, $p70^{S6K}$, and $pp70^{S6K}$ .

the activation by TSH and M22 of the IL-6 gene (14). To identify pathways related to TSH-induced PTX-3 expression, inhibitors of several pathways were screened for their effects. These included AKTi (1 $\mu$M, AKT), LY294002 (10 $\mu$M, PI3K), AG490 (75 $\mu$M, JAK2), and rapamycin (20 nM, mammalian target of rapamycin [mTOR]). Cultures were pretreated without or with one of these inhibitors, and then some wells were treated with bTSH (5 mIU/mL) for 6 hours (Figure 5A) or 90 minutes (Figure 5B and C). The induction of PTX-3 mRNA was substantially attenuated by all 4 inhibitors (Figure 5A). bTSH treatment of fibrocytes resulted in the phosphorylation of AKT, $p70^{S6K}$, and JAK2 (Figure 5B and C). AKTi and LY294002 dampened the formation of pAKT after treatment with bTSH, rapamycin blocked $pp70^{S6K}$ accumulation, and AG490 attenuated pJAK2 (Figure 5B and C). Importantly, the morphology and viability of the fibrocytes were unaffected by these treatments. Thus, it would appear that the activation of multiple pathways is required for maximal induction of PTX-3 by bTSH in fibrocytes.

### TSH increases PTX-3 mRNA stability in fibrocytes

The activity of the PTX-3 gene promoter was examined by first cloning a 1402-bp fragment extending from −1399 to +3 nt and generating a series of deletional mutants of 1128 bp (−1125 to +3 nt), 862 bp (−859 to +3 nt), 592 bp (−589 to +3 nt), and 337 bp (−334 to +3 nt). Each of these was fused to a luciferase reporter and transiently transfected to fibrocytes. As Figure 6A demonstrates, compared with the empty (control) vector, the basal (non-TSH-treated) 1402-bp PTX-3 promoter construct activity was substantial (32.3-fold, $P < .0001$). bTSH failed to consistently influence its activity or that of the shorter fragments. The pattern of basal activities of these truncated fragments suggests that an inducer site might be present in the sequence extending from −1399 to −1125 nt and that a repressor site may be harbored between −859 and −589 nt.

An absence of effects of bTSH on gene promoter activities suggested that PTX-3 mRNA stability might be involved. As Figure 6B indicates, bTSH substantially enhanced survival of the transcript compared with that of untreated fibrocytes. When untreated, PTX-3 mRNA exhibited a $t_{1/2}$ of approximately 3 hours. In the presence of bTSH, the transcript remained stable for the duration of the study (8 hours).

Whether induction by TSH of PTX-3 in fibrocytes is primary or is mediated through the up-regulation of an intermediate protein(s) was next addressed. Fibrocytes were treated without or with cycloheximide (an inhibitor of protein synthesis, 10 $\mu$g/mL) alone or in combination with bTSH for 6 hours. PTX-3 mRNA was modestly induced by cycloheximide as a single agent (1.6-fold) (Figure 6C). bTSH up-regulated the transcript by 6.9-fold when added alone. The combination of cycloheximide and bTSH resulted in a PTX-3 mRNA 15.5-fold above baseline ($P < .0001$ vs bTSH alone). Thus, in fibrocytes, PTX-3 appears to be acting as an immediate early gene product and its induction by TSH does not require intermediate protein synthesis.

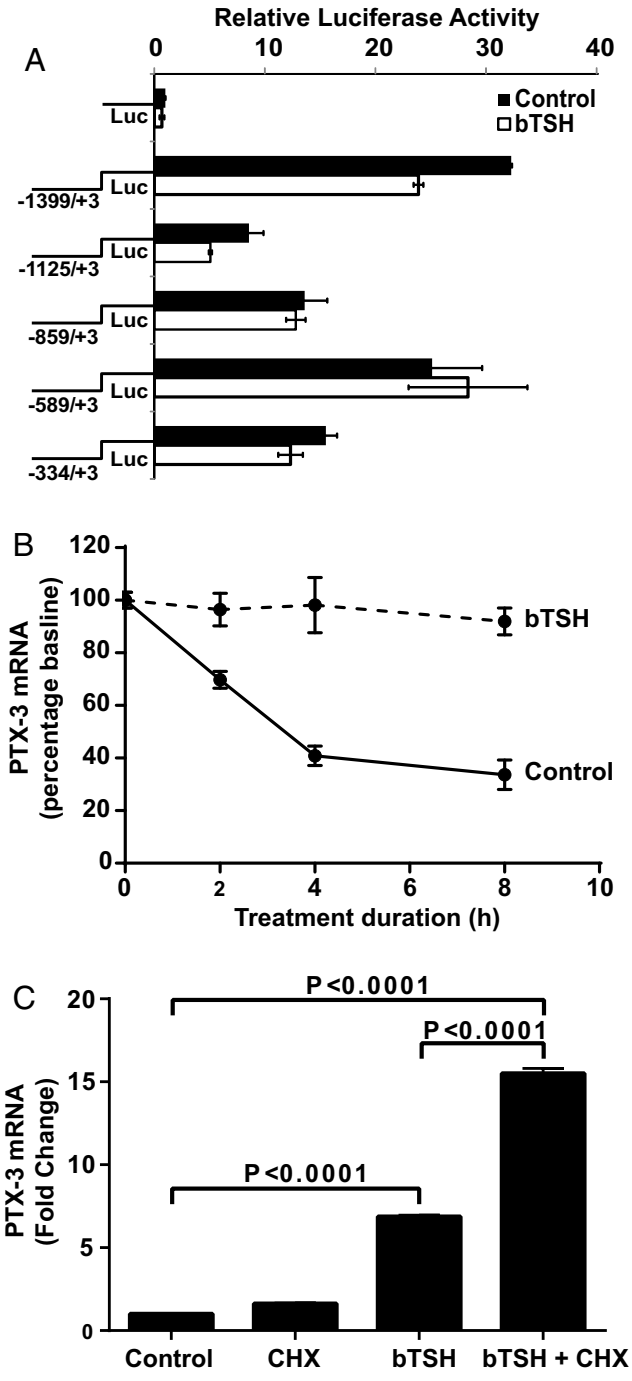


**Figure 6.** Effects of bTSH on PTX-3 gene promoter activity and mRNA stability, and its dependence on intermediate protein synthesis in fibrocytes. A, PTX3 gene promoter-reporter constructs were transfected into fibrocytes as described in *Materials and Methods*. Cultures were treated with nothing or bTSH (5 mIU/mL) for 2 hours, harvested, and luciferase (LUC) activity was determined. B, bTSH (5 mIU/mL) was added to the medium of confluent cell layers for 6 hours and replaced with fresh medium containing DRB (50 $\mu$M) without or with bTSH (5 mIU/mL). RNA was harvested at the times indicated along the abscissa and subjected to RT-PCR for PTX-3 mRNA. C, Confluent cultures were pretreated with cycloheximide (CHX) (10 $\mu$g/mL) for 1 hour and then treated alone or in combination with bTSH (5 mIU/mL) for 6 hours. RNA was extracted and subjected to RT-PCR for PTX-3 mRNA. Data are expressed as means ± SD of triplicates from 3 independent experiments.

## Discussion

PTX-3 is a protein containing 381 amino acids with a predicted molecular mass of 40 kDa (27). The C terminus of PTX-3 shares identity with CRP and SAP, including a pentraxin consensus motif, also known as the "pentraxin signature" (28). Previous studies have shown constitutive expression of PTX-3 protein by neutrophils (22), renal mesangial cells (29), proximal tubular epithelial cells (30), and human amniotic membrane cells (31). Here we provide the first evidence that fibrocytes represent another cell type expressing and secreting PTX-3 (Figure 1).

Recently, several lines of evidence have shown that PTX-3 has nonredundant roles in inflammation (32), extracellular matrix deposition (33), and neovascularization (34). Zhang et al (31) observed that PTX-3 formed a complex with hyaluronan. Because these processes are intimately involved in the tissue remodeling associated with TAO, it is possible that PTX-3 may have some role in the disease pathogenesis. Earlier studies detected PTX-3 expression in orbital connective tissues in active TAO (24). Whether the molecule might be targeted in some aspect of therapy is as yet uncertain and will require greater insight into whether its levels of expression bear a relationship with disease activity and severity. The answer probably rests on whether orbit-specific delivery of modulatory agents is possible.

Mechanisms involved in the regulation of PTX-3 expression appear to be complex and both cell type and inducer specific. Fibrocytes express considerably higher levels of cell surface TSHR than do GD-OFs (8, 9). Yet no consistent differences emerge from these studies regarding the magnitude of PTX-3 induction between the 2 cell types. Induction of PTX-3 by TSH in fibrocytes results from the enhanced PTX-3 mRNA stability, but no effects could be detected on the activity of the PTX-3 gene promoter. Precedents exist for both transcriptional and post-transcriptional regulation of PTX-3 expression. The current findings diverge from those of Basile et al (35), who demonstrated increased human promoter-reporter activity in transfected human fibroblasts treated with TNF-$\alpha$ and IL-1$\beta$. In contrast, IL-6 failed to alter promoter activity. That same study examined activity in transfected Hep 3B hepatoma cells and found that neither TNF-$\alpha$ nor IL-1$\beta$ influenced promoter activity. With regard to regulating PTX-3 mRNA stability, Polentarutti et al (36) demonstrated that interferon-$\gamma$ could inhibit IL-1$\beta$-induced PTX-3 expression in monocytes through PTX-3 mRNA destabilization. Prostaglandin $E_2$ and the 3′ untranslated region of CCAAT/enhancer binding protein enhance PTX-3 promoter activities in THP-1 cells (37). Other studies have demonstrated the importance of methylation

states as a determinant of PTX-3 expression (38). Thus, both transcriptional and posttranscriptional levels of control appear to be involved in the expression of PTX-3 in a cell-specific manner.

Our studies suggest that a higher concentration of M22 may be necessary for the induction of PTX-3 than that required for provoking the phosphorylation of Akt in GD-OFs (10–50 ng/mL) (39). The basis for this apparent shift in the dose-response curve is uncertain. Our findings point to the central involvement of the PI3K/Akt/FKBP-rapamycin-associated protein /mTOR/$p70^{s6k}$ pathway in mediating the induction by TSH of PTX-3, based on its sensitivity to multiple small molecule inhibitors of several of the kinases in that signaling complex (Figure 5). These findings are congruent with earlier studies from our group demonstrating the importance of this pathway in signaling downstream from IGF-IR and TSHR in fibrocytes and OFs (14, 40). This pathway is a key participant in the activation of survival genes and has been implicated in several diseases such as cancer (41). Further, it is critical to many responses mediated through both receptors (40, 42).

Several laboratory groups, including our own, have reported divergent phenotypes exhibited by OFs and fibrocytes coming from donors with GD and TAO compared with those from healthy individuals. It appears that the induction by TSH of PTX-3 differs from those examples in that the cellular response is similar regardless of the donor's health status. Further, this induction does not seem to be cell type specific in that both exhibit this response. Thus, the involvement of the TSH/TSHR pathway in the regulation of PTX-3 might be generalizable to multiple tissues and organ systems. Further studies will be required to determine whether this scenario is correct.

Our earlier studies have disclosed that TSHR can form a physical and functional complex with IGF-IR (43). Teprotumumab, a monoclonal IGF-IR blocking antibody, attenuated the induction of PTX-3 as did 1H7, another blocking antibody. These findings underscore the potential therapeutic benefit of interrupting the IGF-IR pathway in TAO. Clearly, additional studies, including those interrupting PTX-3 expression and determining its consequences on the fibrocyte and fibroblast phenotype will be necessary to more fully understand the role of this protein on cellular function. However, the current findings identify the protein as a member of the TSHR response repertoire in fibrocytes. They suggest that it might play a fundamental role in determining both the magnitude and qualitative aspects of connective tissue remodeling, which could apply to the pathogenesis of TAO and other fibrocyte-related disease processes. The report from Gomer and colleagues (44) that SAP is a powerful inhibitor of fibrocyte differentiation raises potentially interesting questions about what role, if any, PTX-3 might play in determining its developmental fate. A very recent publication by this same group has defined a role for PTX-3 in promoting fibrocyte differentiation (45).

## Acknowledgments

Address all correspondence and requests for reprints to: Terry J. Smith, MD, Department of Ophthalmology and Visual Sciences, University of Michigan Medical School, Kellogg Eye Center, Brehm Tower, 1000 Wall Street, Ann Arbor, MI 48105. E-mail: terrysmi@med.umich.edu.

This work was supported in part by National Institutes of Health Grant EY008976, Center for Vision Grant EY007003 from the National Eye Institute, an unrestricted grant from Research to Prevent Blindness, and the Bell Charitable Foundation.

Disclosure Summary: The authors have nothing to disclose.

## References

1. **Brent GA.** Clinical practice. Graves' disease. *N Engl J Med*. 2008; 358:2594–2605.
2. **Gianoukakis AG, Khadavi N, Smith TJ.** Cytokines, Graves' disease, and thyroid-associated ophthalmopathy. *Thyroid*. 2008;18:953–958.
3. **Regensburg NI, Wiersinga WM, Berendschot TT, Potgieser P, Mourits MP.** Do subtypes of graves' orbitopathy exist? *Ophthalmology*. 2011;118:191–196.
4. **Kazim, M, Goldberg RA, Smith TJ.** Insights into the pathogenesis of thyroid-associated orbitopathy: evolving rationale for therapy. *Arch Ophthalmol*. 2002;120:380–386.
5. **Smith TJ.** Novel aspects of orbital fibroblast pathology. *J Endocrinol Invest*. 2004;27:246–253.
6. **van Steensel L, Dik WA.** The orbital fibroblast: a key player and target for therapy in Graves' ophthalmopathy. *Orbit*. 2010;29:202–206.
7. **Smith TJ.** Fibroblast biology in thyroid diseases. *Curr Opin Endocrinol Diabetes Obes*. 2002;9:393–400.
8. **Douglas RS, Afifiyan NF, Hwang CJ, et al.** Increased generation of fibrocytes in thyroid-associated ophthalmopathy. *J Clin Endocrinol Metab*. 2010;95:430–438.
9. **Smith TJ.** TSH-receptor-expressing fibrocytes and thyroid-associated ophthalmopathy. *Nat Rev Endocrinol*. 2015;11:171–181.
10. **Bucala R, Spiegel LA, Chesney J, Hogan M, Cerami A.** Circulating fibrocytes define a new leukocyte subpopulation that mediates tissue repair. *Mol Med*. 1994;1:71–81.
11. **Pilling D, Fan T, Huang D, Kaul B, Gomer RH.** Identification of markers that distinguish monocyte-derived fibrocytes from monocytes, macrophages, and fibroblasts. *PLoS One*. 2009;4:e7475.
12. **Bellini A, Mattoli S.** The role of the fibrocyte, a bone marrow-derived mesenchymal progenitor, in reactive and reparative fibroses. *Lab Invest*. 2007;87:858–870.
13. **Fernando R, Atkins S, Raychaudhuri N, et al.** Human fibrocytes coexpress thyroglobulin and thyrotropin receptor. *Proc Natl Acad Sci U S A*. 2012;109:7427–7432.
14. **Raychaudhuri N, Fernando R, Smith TJ.** Thyrotropin regulates IL-6 expression in $CD34^+$ fibrocytes: clear delineation of its cAMP-independent actions. *PLoS One*. 2013;8:e75100.
15. **Fernando R, Vonberg A, Atkins SJ, Pietropaolo S, Pietropaolo M, Smith TJ.** Human fibrocytes express multiple antigens associated

with autoimmune endocrine diseases. *J Clin Endocrinol Metab*. 2014;99:E796–E803.
16. **Gillespie EF, Papageorgiou KI, Fernando R, et al.** Increased expression of TSH receptor by fibrocytes in thyroid-associated ophthalmopathy leads to chemokine production. *J Clin Endocrinol Metab*. 2012;97:E740–E746.
17. **Alles VV, Bottazzi B, Peri G, Golay J, Introna M, Mantovani A.** Inducible expression of PTX3, a new member of the pentraxin family, in human mononuclear phagocytes. *Blood*. 1994;84:3483–3493.
18. **Tong M, Carrero JJ, Qureshi AR, et al.** Plasma pentraxin 3 in patients with chronic kidney disease: associations with renal function, protein-energy wasting, cardiovascular disease, and mortality. *Clin J Am Soc Nephrol*. 2007;2:889–897.
19. **Klouche M, Peri G, Knabbe C, et al.** Modified atherogenic lipoproteins induce expression of pentraxin-3 by human vascular smooth muscle cells. *Atherosclerosis*. 2004;175:221–228.
20. **Mantovani A, Garlanda C, Bottazzi B, et al.** The long pentraxin PTX3 in vascular pathology. *Vascul Pharmacol*. 2006;45:326–330.
21. **Rutkowski MJ, Sughrue ME, Kane AJ, Mills SA, Parsa AT.** Cancer and the complement cascade. *Mol Cancer Res*. 2010;8:1453–1465.
22. **Jaillon S, Peri G, Delneste Y, et al.** The humoral pattern recognition receptor PTX3 is stored in neutrophil granules and localizes in extracellular traps. *J Exp Med*. 2007;204:793–804.
23. **Presta M, Camozzi M, Salvatori G, Rusnati M.** Role of the soluble pattern recognition receptor PTX3 in vascular biology. *J Cell Mol Med*. 2007;11:723–738.
24. **Planck T, Parikh H, Brorson H, et al.** Gene expression in Graves' ophthalmopathy and arm lymphedema: similarities and differences. *Thyroid*. 2011;21:663–674.
25. **Smith TJ, Sempowski GD, Wang HS, Del Vecchio PJ, Lippe SD, Phipps RP.** Evidence for cellular heterogeneity in primary cultures of human orbital fibroblasts. *J Clin Endocrinol Metab*. 1995;80:2620–2625.
26. **Chen H, Mester T, Raychaudhuri N, et al.** Teprotumumab, an IGF-1R blocking monoclonal antibody inhibits TSH and IGF-1 action in fibrocytes. *J Clin Endocrinol Metab*. 2014;99:E1635–E1640.
27. **Breviario F, d'Aniello EM, Golay J, et al.** Interleukin-1-inducible genes in endothelial cells. Cloning of a new gene related to C-reactive protein and serum amyloid P component. *J Biol Chem*. 1992;267:22190–22197.
28. **Bottazzi B, Vouret-Craviari V, Bastone A, et al.** Multimer formation and ligand recognition by the long pentraxin PTX3. Similarities and differences with the short pentraxins C-reactive protein and serum amyloid P component. *J Biol Chem*. 1997;272:32817–32823.
29. **Bussolati B, Peri G, Salvidio G, Verzola D, Mantovani A, Camussi G.** The long pentraxin PTX3 is synthesized in IgA glomerulonephritis and activates mesangial cells. *J Immunol*. 2003;170:1466–1472.
30. **Nauta AJ, de Haij S, Bottazzi B, et al.** Human renal epithelial cells produce the long pentraxin PTX3. *Kidney Int*. 2005;67:543–553.
31. **Zhang S, Zhu YT, Chen SY, He H, Tseng SC.** Constitutive expression of pentraxin 3 (PTX3) protein by human amniotic membrane cells leads to formation of the heavy chain (HC)-hyaluronan (HA)-PTX3 complex. *J Biol Chem*. 2014;289:13531–13542.
32. **Padeh S, Farzam N, Chayen G, Gerstein M, Berkun Y.** Pentraxin 3 is a marker of early joint inflammation in patients with juvenile idiopathic arthritis. *Immunol Res*. 2013;56:444–450.
33. **Inforzato A, Rivieccio V, Morreale AP, et al.** Structural characterization of PTX3 disulfide bond network and its multimeric status in cumulus matrix organization. *J Biol Chem*. 2008;283:10147–10161.
34. **Mantovani A, Garlanda C, Doni A, Bottazzi B.** Pentraxins in innate immunity: from C-reactive protein to the long pentraxin PTX3. *J Clin Immunol*. 2008;28:1–13.
35. **Basile A, Sica A, d'Aniello E, et al.** Characterization of the promoter for the human long pentraxin PTX3. Role of NF-$\kappa$B in tumor necrosis factor-$\alpha$ and interleukin-1$\beta$ regulation. *J Biol Chem*. 1997;272:8172–8178.
36. **Polentarutti N, Picardi G, Basile A, et al.** Interferon-$\gamma$ inhibits expression of the long pentraxin PTX3 in human monocytes. *Eur J Immunol*. 1998;28:496–501.
37. **Hsiao YW, Li CF, Chi JY, et al.** CCAAT/enhancer binding protein delta in macrophages contributes to immunosuppression and inhibits phagocytosis in nasopharyngeal carcinoma. *Sci Signal*. 2013;6:ra59.
38. **Wang JX, He YL, Zhu ST, et al.** Aberrant methylation of the 3q25 tumor suppressor gene PTX3 in human esophageal squamous cell carcinoma. *World J Gastroenterol*. 2011;17:4225–4230.
39. **Kumar S, Nadeem S, Stan MN, Coenen M, Bahn RS.** A stimulatory TSH receptor antibody enhances adipogenesis via phosphoinositide 3-kinase activation in orbital preadipocytes from patients with Graves' ophthalmopathy. *J Mol Endocrinol*. 2011;46:155–1163.
40. **Pritchard J, Horst N, Cruikshank W, Smith TJ.** Igs from patients with Graves' disease induce the expression of T cell chemoattractants in their fibroblasts. *J Immunol*. 2002;168:942–950.
41. **Porta C, Paglino C, Mosca A.** Targeting PI3K/Akt/mTOR signaling in cancer. *Front Oncol*. 2014;4:64.
42. **Suh JM, Song JH, Kim DW, et al.** Regulation of the phosphatidylinositol 3-kinase, Akt/protein kinase B, FRAP/mammalian target of rapamycin, and ribosomal S6 kinase 1 signal pathways by thyroid-stimulating hormone (TSH) and stimulating TSH receptor antibodies in the thyroid gland. *J Biol Chem*. 2003;278:21960–21971.
43. **Tsui S, Naik V, Hoa N, et al.** Evidence for an association between thyroid-stimulating hormone and insulin-like growth factor 1 receptors: a tale of two antigens implicated in Graves' disease. *J Immunol*. 2008;181:4397–4405.
44. **Pilling D, Buckley CD, Salmon M, Gomer RH.** Inhibition of fibrocyte differentiation by serum amyloid P. *J Immunol*. 2003;171:5537–5546.
45. **Pilling D, Cox N, Vakil V, Verbeek JS, Gomer RH.** The long pentraxin PTX-3 promotes fibrocyte differentiation. *PLoS One*. 2015;10:e0119709.